*Physicochem. Probl. Miner. Process. 53(1), 2017, 628−643*

www.minproc.pwr.wroc.pl/journal

Physicochemical Problems of Mineral Processing

ISSN 1643-1049 (print)
ISSN 2084-4735 (online)

*Received December 2, 2015; reviewed; accepted March 15, 2016*

# A COMPARISON OF REMOVAL OF UNBURNED CARBON FROM COAL FLY ASH USING A TRADITIONAL FLOTATION CELL AND A NEW FLOTATION COLUMN

**Ming XU[*], Haijun ZHANG[**], Changqing LIU[*], Yi RU[*], Guosheng LI[*], Yijun CAO[**]**

[*] School of Chemical Engineering and Technology, China University of Mining and Technology, Xuzhou 221116, China

[**] National Engineering Research Center for Coal Processing and Purification, China University of Mining and Technology, Xuzhou 221116, China, corresponding author, zhjcumt@163.com

**Abstract:** The purpose of this study was to investigate the performance of a new cyclonic-static micro-bubble flotation column for removal of unburned carbon from coal fly ash compared with a traditional flotation cell. The coal fly ash samples and flotation products were characterized by the size fraction, X-ray diffraction, X-ray fluorescence, contact angle measurements and scanning electron microscopy. Under optimal flotation conditions, the performance comparison between the flotation column and the traditional mechanical flotation cell showed that the recovery of unburned carbon in the flotation column was equal to 89.69%, and was 6.5% greater than the recovery in the traditional flotation cell. The loss-on-ignition of the tailing in the flotation column decreased to 1.99%, and was 1.1% lower than in the traditional flotation cell. The size and scanning electron microscope analyses of the products demonstrated that the flotation column was beneficial for the recovery of fine particles. The recovery advantages of the cyclonic-static micro-bubble flotation column of unburned carbon from the coal fly ash were mainly attributed to the pipe flow mineralization and cyclonic mineralization.

***Keywords:*** *coal fly ash, unburned carbon, flotation cell, flotation column*

## Introduction

Coal fly ash is a major solid product of thermal power plants that is fine and powdery. It can cause pollution if discharged into the environment. The most immediate environmental concern is the way of using coal fly ash. Coal fly ash is also used in cement production. The presence of the unburned carbon in fly ash will decrease the compressive strength of the cement. The standard specification of 1$^{st}$ grade fly ash in China limits the loss-on-ignition (LOI) values less than 5% assuming that this parameter provides good estimation of carbon content. However, the LOI of most

http://dx.doi.org/10.5277/ppmp170149

China thermal power plants fly ash is in the range of 15%-20% (Huang et al., 2003; Asokan et al., 2005; Sahbaz et al., 2008; Lee, et al. 2010). Thus, removing the unburned carbon from coal fly ash is the key for its utilization. Unburned carbon is typically removed by either electrostatic separation, gravitational separation or froth flotation. Froth flotation exploits the differences in surface hydrophobicity of the different constituent minerals and selectively separates the valuable minerals from gangue by attaching them to air bubbles and recovering them from the mineral froth. Many studies show that froth flotation is the most efficient and economic method for the removal of unburned carbon (Demir et al., 2008; Altun et al., 2009; Ucurum, 2009; McCarthy et al., 2013).

Froth flotation is a common process in the minerals separation industry, and the process is increasingly used in waste treatment. The most widely used equipment is the traditional flotation cell. Additionally, new flotation technologies have developed rapidly and become an important way to treat fine minerals (Tao et al., 2000; Martinez and Uribe, 2008; Tasdemir et al., 2011; Nakhaei and Irannajad, 2013; Han et al., 2014; Ucar et al., 2014; Kowalczuk et al., 2015; Gursoy and Oteyaka, 2015). Due to the low collision efficiency, the flotation efficiency for fine carbon particles is poor (Miettinen et al., 2010). However, the particle size of most thermal power plants fly ash in China is fine. Thus, the key to reduce the LOI of the fly ash is to recover the fine unburned carbon particles.

A cyclonic-static micro-bubble flotation column (FCSMC), as shown in Fig. 1, features multiple mineralization steps, including counter-current, cyclone and pipe flow mineralization, in a single column (Cao et al., 2009; Li et al., 2009; Deng et al., 2013; Zhang et al., 2013). Counter-current mineralization was realized to generate a high-quality concentrate from raw materials. One of the advantages of counter-current mineralization was that it gave a longer mineralization section than a conventional cell. This increased the residence time of particles in the mineralization process which allowed entrained gangue particles to be drained back to the pulp. Subsequently, cyclone mineralization in the cyclone separation step further separated flotation middling to obtain high-quality tailings. Cyclone mineralization increased the probability of collision between the particles and bubbles and forcibly recover the floating minerals depending on the high-intensity centrifugal force field and the abundant bubbles in the cyclone section. Finally, pipe flow mineralization was used for separation of the cyclone middling and circulation of pulp. Pipe flow mineralization inhaled and crushed air into micro-bubbles and produced strong turbulence which increased the probability of collision between the particles and bubbles, especially for fine particles (Li et al., 2010; Yan et al., 2012; Zhang et al., 2013). The process also showed major advantages compared with traditional flotation cells, including requiring less physical space and power in addition to having a greater ability to recover more valuable fine particles (Li et al., 2012; Zhang et al., 2013).

In this paper, to further evaluate the flotation performance of FCSMC for the removal of unburned carbon from coal fly ash, flotation experiments are conducted in

a laboratory-scale FCSMC system and traditional flotation cell. The flotation performance for removing unburned carbon from coal fly ash is compared under the optimum conditions between the FCSCM and traditional flotation cell. Additionally, the effects of pipe-flow minimization and cyclonic minimization of FCSMC are analysed.

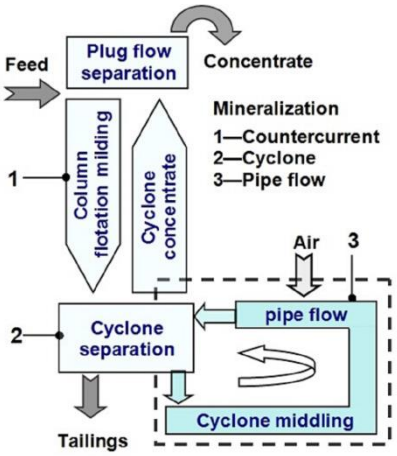


Fig. 1. Schematic drawing of the cyclonic-static micro-bubble flotation column (Zhang et al., 2013)

## Experimental

### Materials and sample preparation

Coal fly ash was obtained from the thermal power plant in the ShanXi Province, China. The samples were blended and then placed in plastic bags and stored in an icebox. The moisture content of the prepared samples was 10%. Loss-on-ignition (LOI) analyses were conducted with moisture-free fly ash samples that were dried in a laboratory furnace. Light diesel oil was used as the collector, a 730-flotation reagent prepared by mixing polyethylene glycol and 2-Octanol was used as the frother.

### Experimental methods and procedures

#### Traditional flotation cell experiments

The traditional flotation cell experiments were performed in a 1.5 $dm^3$ mechanical flotation cell at a solids concentration of 20%. In each test, the sample was mixed with tap water and light diesel oil in the machine and was agitated for 7 min. Then, the frother was added to the slurry in succession. The conditioning time of the frother was 5 min. After the conditioning process, the desired amount of tap water was added to increase the volume of the pulp in the machine to 1.5 $dm^3$. Subsequently, air was introduced into the machine, the air-flow rate was 0.2 $m^3/h$. Tap water was added as

necessary to maintain a constant pulp level, and the pulp was then floated for 4 min, because of the LOI of the tailing kept almost unchanged as the time prolong. All of the tests were conducted at the natural pH value (~7). The flotation concentrate and the tailings were filtered, dried and weighed.

**New flotation column experiments**

The flotation column experiments were conducted with a laboratory-scale cyclonic-static micro-bubble flotation column (FCSMC). Five parts constitute the system, as shown in Fig. 2, including the mixing tank, feed pump, flotation column, circulation pump and tailings pump. The conditioning process was the same as the traditional flotation cell tests in the mixing tank. The FCSMC device is in the form of a single column, which is composed of Plexiglas that has a diameter of 50 mm and height of 2000 mm. It consists of the column flotation section, cyclone separation section and pipe flow section. The column flotation section provides the low-turbulence environment for counter-current mineralization. Below the flotation section is the cyclone separation section, which provides the environment for cyclone mineralization depending on the high-intensity centrifugal force field. The cyclone separation section flows into the pipe flow section through a circulation pump, and the poor floatability particle enhances mineralization in the pipe flow section. Cyclonic separation requires a tangent feed, so the pipe flow section is connected perpendicularly to the cyclone separation in a tangent direction. An external bubble generator to inhale and crush air into micro-bubbles is installed at the pipe flow mineralization section, which provides the environment for pipe flow mineralization (Zhang et al., 2013).

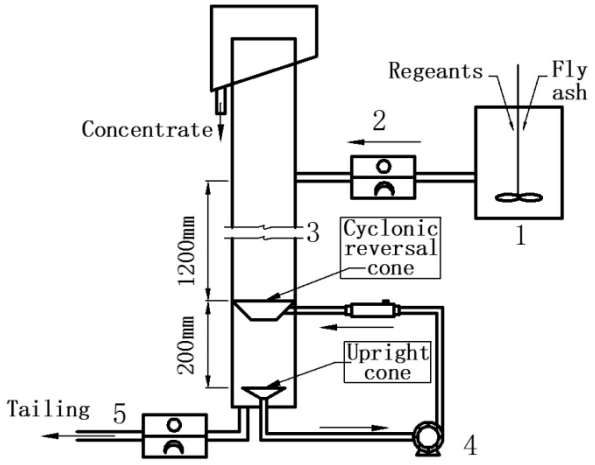


Fig. 2. Schematic illustration of a specially designed column for the study:
1. mixing tank; 2. feed peristaltic pump; 3. flotation column;
4. circulation pump; 5. tailing peristaltic pump

**XRD and XRF analysis**

A BrukerD8 Advance X-ray diffractometer was used for the elemental analysis to obtain the mineralogical composition of the sample. A chemical composition analysis of the sample was completed using a S8 TIGER X-ray fluorescence analyser.

**Particle size analysis**

A SPB200 vibrating Taylor screen was used for the size analysis to obtain the yield and LOI of different particle size fractions. The decreasing order of mesh apertures was 300, 125, 74, and 45 μm. The samples were weighed and submitted to measure for LOI.

**Contact angle measurements**

It is difficult to obtain a low ash content product with sink-and-float testing because the -45 μm sized class particles in the coal fly ash tend to have high viscosity. Thus, a vibrating Taylor screen was used to remove the -45 μm sized class particle. Then, the samples were submitted to a sink-and-float test to obtain different fraction density products. Each density product was washed, filtered, dried and weighed. Then, some of the samples were used for ash content analysis. A DSA100 (Kruss) goniometer was used to conduct the contact angle analysis of different density products. Each density product was pressed under a pressure of approximate 2500 psi (17.22 GPa) using a tablet machine for 2 min to form a pellet. Each result was measured three times, and an average contact angle was calculated. Values of the contact angle were determined by captured image of a droplet. Building on the digital images of the droplets, geometrical approach and developed tangent method were applied. Depending on the level of wettability, Young-Laplace formulas were used in geometrical approach, which named contour image analysis method.

**SEM analysis**

A FEI Quanta 250 SEM in addition to an energy dispersive X-ray (EDX) was used to analyze the morphology and to locate the chemical element of interest of the fly ash. The chemical analysis was provided in colored EDX images. In the colored pictures, different colors represent different elements.

## Results and discussion

### Coal fly ash characterization

The XRD results presented in Fig. 3 indicate that the main crystalline substance in the sample is mullite, and a small amount of quartz, illite and gypsum are also presented. In the fly ash, the amount of glass and cenosphere production is related to the illite content of the coal, however the mullite content of the fly ash is linked to kaolinite in the coal sample (Spears, 2000). The content of $Al_2O_3$, $SiO_2$, $Fe_2O_3$ and CaO in the sample is 27.29%, 41.03%, 4.54% and 6.47%, respectively, as shown in Table 1. The fly ash sample having $SiO_2 + Al_2O_3 + Fe_2O_3$, of which content is greater than 70% and

CaO less than 10%, belongs to F class. The SEM and SEM-EDX micrographs of raw fly ash are shown in Fig. 4, the magnification time was fixed at 800. As shown in the picture, yellow and green represent carbon element and calcium element, respectively. XRD and XRF analyses show that there is no mineral that contains carbon element except unburned carbon, thus the particles are unburned carbon colored in yellow. Similarly, only gypsum contain the calcium element. The irregular particles labelled 1 are unburned carbon, and the regular quadrate particles labelled 2 are gypsum. The globular particles are mullite.

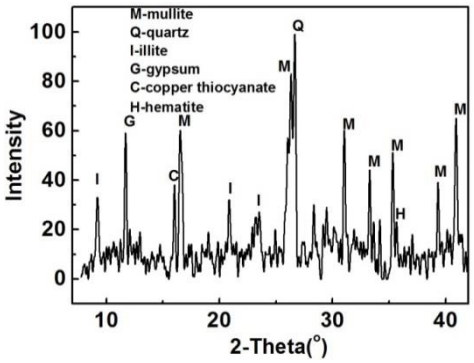


Fig. 3. XRD diffractograms of the sample

It can be clearly seen from the particle size analysis results (Table 2) that the yield of the −74 μm sized fraction is 82.03%, noting that the yield of the −45 μm sized fraction is 61.79%. The size distribution of the unburned carbon makes it obvious that roughly 64.7% of the total is in the −74 μm sized fraction. Due to the low probability of bubble-particle collision, the recovery of fine particles is low in flotation (Shahbazi et al., 2010; Chipfunhu et al., 2012). Thus, the highly efficient mineralization of the fine particles is the key for improving the recovery of unburned carbon.

The contact angle is an important parameter to reflect the particle hydrophobicity (Ozdemir et al., 2009; Xia and Yang, 2013; Zou, 2013). Table 3 gives the contact angle measurement results of the coal fly ash particles with different density and ash contents. It is obvious that the hydrophobicity property of the coal fly ash is poor. The contact angle decreases as the density of the coal fly ash increases, except for the fraction of -1.4 g/cm$^3$. Smaller contact angle of the fraction of -1.4 g/cm$^3$ could be caused by coal fly ash cenosphere that was transferred into the product. Fly ash cenosphere is spherical silica-alumina particles, and it possesses the favourable characteristics of having a density close to the density of water and high strength (Pang et al., 2011; Kiani et al., 2015; Wang et al., 2015). Except for the fraction of -1.4 g/cm$^3$, the largest contact angle of the coal fly ash is 32.8$^o$, and the smallest contact angle of the coal fly ash is 13.6$^o$, as shown in Fig. 5. Oxidation is an important factor causing a significant decrease in hydrophobicity level of coals. The fly ash used in the present study is a coal burned product. Due to the severe oxidation of the unburned

carbon surface, the hydrophobicity of the unburned carbon is so poor result in the contact angle of the unburned carbon is small (Huang et al., 2003; Sahbaz et al., 2008). This indicates that the bubble-particle collisions and adhesion in the slurry are difficult and that the unburned carbon in the coal fly ash is difficult to float.

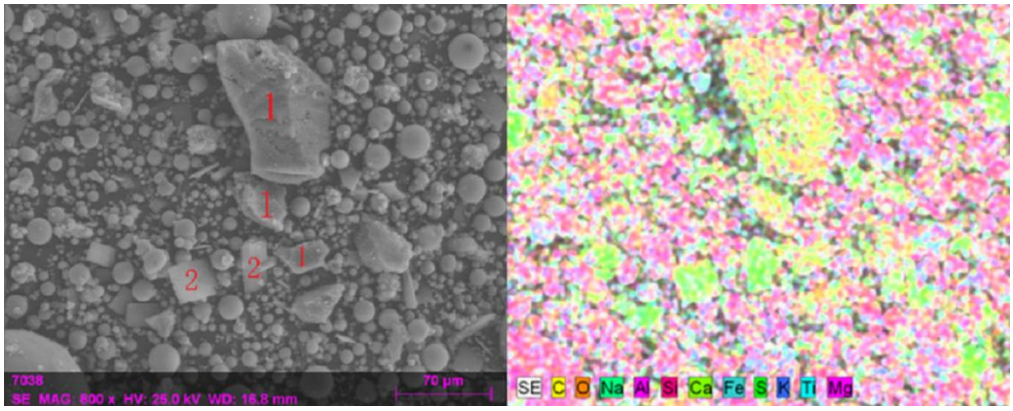


Fig. 4. SEM and SEM-EDX results for fly ash, 1-unburned carbon, 2-gypsum

Table 1. Chemical composition of fly ash sample

| Chemical composition | Amount (%) |
|---|---|
| $Na_2O$ | 0.67 |
| MgO | 0.99 |
| $K_2O$ | 1.20 |
| $Ti_2O$ | 1.34 |
| S | 2.61 |
| $Fe_2O_3$ | 4.54 |
| CaO | 6.47 |
| $Al_2O_3$ | 27.29 |
| $SiO_2$ | 41.03 |
| Other | 13.85 |

Table 2. Particle size and unburned carbon analysis of the as-received fly ash sample

| Size fraction (μm) | Yield (%) | LOI (%) | Unburned carbon distribution (%) |
|---|---|---|---|
| +300 | 0.58 | 20.41 | 1.00 |
| -300+125 | 4.52 | 22.01 | 8.38 |
| -125+74 | 12.87 | 23.91 | 25.92 |
| -74+45 | 20.24 | 21.65 | 36.91 |
| -45 | 61.79 | 5.34 | 27.79 |
| Total | 100.00 | 11.87 | 100.00 |

Table 3. Contact angles of different density fractions of unburned carbon

| Density fraction (g/cm$^3$) | Yield (%) | Ash content (%) | Contact angle (°) |
|---|---|---|---|
| -1.4 | 2.73 | 73.19 | 23.3 |
| 1.4～1.5 | 10.63 | 32.23 | 32.8 |
| 1.5～1.6 | 12.35 | 34.14 | 30.5 |
| 1.6～1.8 | 12.16 | 53.13 | 25.6 |
| 1.8～2.0 | 6.85 | 82.94 | 21.8 |
| +2.0 | 55.28 | 98.65 | 13.6 |
| Total | 100.00 | 76.14 | |

**Removal performance of unburned carbon**

During testing removal of the unburned carbon from the coal fly ash, the performance of separation equipment is generally determined by evaluating the loss-on-ignition of the tailing ($L_t$) (%) and the removal rate of unburned carbon (*RUC*) (%). These values are calculated using the following formulas:

$$L_t = 100 - A_t \tag{1}$$

$$RUC = \frac{\gamma_c L_c}{L_f} \times 100 \tag{2}$$

where $A_t$ is the ash content of the tailing (%), $\gamma_c$ is the yield of the concentrate (%), $L_c$ is the LOI of the concentrate (%), and $L_f$ is the LOI of the feed (%). The local separation efficiency ($S_e$) of the process is defined as the recovery of the useful minerals minus the recovery of the not useful minerals (Han et al., 2014), which for removing unburned carbon from coal fly ash is given as:

$$S_e = \frac{\gamma_c}{L_f} \times \frac{L_c - L_f}{100 - L_f} \times 100 \tag{3}$$

In this paper, the above performance measures were used to quantify the effects of the traditional flotation cell and flotation column. $L_t$, as a major factor, determines whether the tailing can be used as cement admixture, which decreased as the *RUC* of the tailing increased. Thus, the flotation parameters were optimized to get lower $L_t$. $S_e$ was used to compare the separation efficiency between the traditional flotation cell and FCSMC.

Figure 6 shows the relationship between LOI and yield of the tailing from the flotation cell and FCSMC. The LOI of the tailing from FCSCM was lower than that of flotation cell for the same yield. By optimizing the flotation parameters, the optimal flotation results can be obtained in the traditional flotation cell and flotation column tests. Figure 7 shows the comparison of the traditional flotation cell and flotation

column performances of the coal fly ash flotation. When the introduced air was 0.4 $m^3$/h, circulating pump pressure 0.06 MPa, collector and frother dosage 1000 g/Mg, *RUC* in the flotation column test 89.69%, $S_e$ 70.13%, yield of the concentrate 28.36%, $L_c$ 41.59% and $L_t$ was 1.99%. When the introduced air was 0.2 $m^3$/h, the rotational speed of flotation cell 2000 rev/min, collector and frother dosage 1000 g/Mg, *RUC* in the traditional flotation cell test 83.15%, $S_e$ 64.39%, yield of the concentrate 27.51%, $L_c$ 41.09% and $L_t$ was 3.16%. *RUC* in the flotation column test was much higher than that in the traditional flotation cell test, and $L_t$ in the flotation column test was much lower than that in the traditional flotation cell test. These results indicate that the flotation column can remove unburned carbon from coal fly ash in a much more complete way compared with the traditional flotation cell. Meanwhile, the value of $S_e$ in the flotation column test is much higher than that in the traditional flotation cell test, indicating that the flotation column performance is better than the traditional flotation cell performance for removing unburned carbon from coal fly ash.

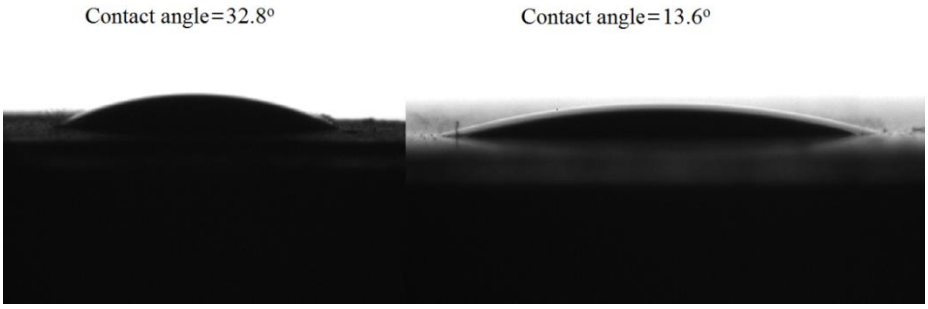


Fig. 5. Comparison of the largest contact angle and smallest contact angle

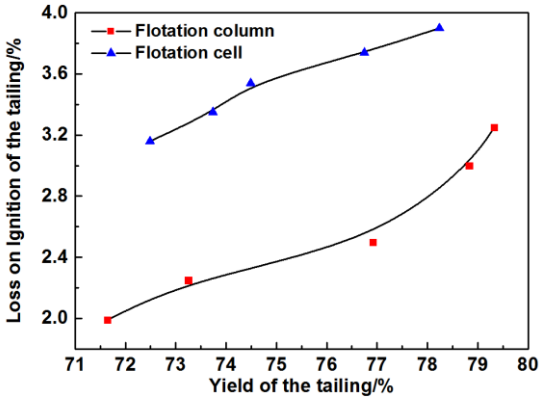


Fig. 6. Relationship between LOI and yield of tailing for flotation cell and FCSMC

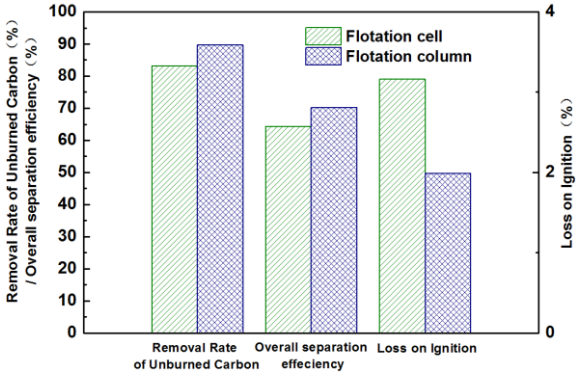


Fig. 7. A comparison of performance in traditional cell and flotation column

## Coal particle recovery

A size analysis of the concentrates by LASER diffraction (S3500) was used to investigate the performance of the different flotation equipment. The results are presented in Fig. 8. The SEM and SEM-EDX images of the tailing products obtained from the traditional flotation cell and flotation column are shown in Fig. 9 and Fig. 10, the magnification time was fixed at 800.

Figure 8 shows the different particle size distributions of the concentrates obtained from the traditional flotation cell and the flotation column. As mentioned above, the ash content in concentrates from the traditional cell and column differs slightly. The differences in the −74 μm sized fractions are obvious. The yield of the −74 μm sized fractions for the flotation column is higher than that of the traditional flotation cell by approximate 6%, confirming that the flotation recovery in the column for the −74 μm sized fractions is higher than that in the traditional flotation cell. The advantage of the flotation column can be explained as follows. It is well studied that the pipe mineralization can inhaled and crushed air into micro-bubbles, and the micro-bubbles can increase the probability of collision and reduce the probability of detachment which can increase the recovery of unburned carbon. In the cyclone mineralization, the centrifugal force field can expand the size fraction range for common fine particle flotation and allow efficient separation of fine particles (Li et al., 2012). It indicates that the efficiency of the flotation column in recovering fine unburned carbon particles from coal fly ash is much higher than that of the traditional flotation cell, particularly when the most unburned carbon is distributed at fine particle sizes in the coal fly ash. This fact is further confirmed as the unburned carbon particle sizes in the tailing products shown in SEM-EDX images. As shown in the picture, the yellow represents carbon element. As the XRD and XRF analyses noted above, there is no mineral that contains carbon element except unburned carbon, thus the particles are unburned carbon majorly colored in yellow. It is clear that some unburned carbon particles exist in the traditional flotation cell image, which were labelled 1, as shown in Fig. 9. The size of these unburned carbon particles is smaller than −74 μm. Conversely, due to the

higher recovery of unburned carbon, it is difficult to observe any unburned carbon particles in the flotation column image, as shown in Fig. 10.

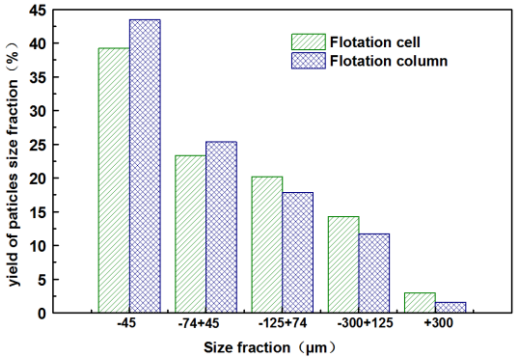


Fig. 8. Yield of concentrate particle size fraction obtained with different flotation equipment

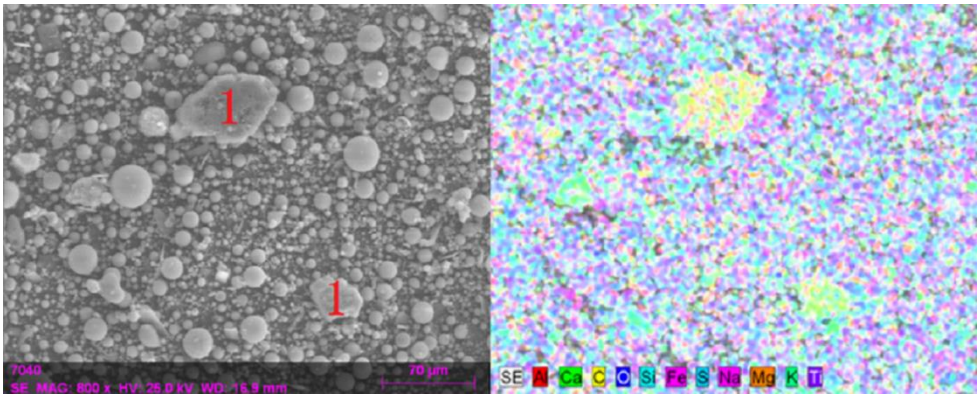


Fig. 9. SEM and SEM-EDX results for traditional flotation cell tailing

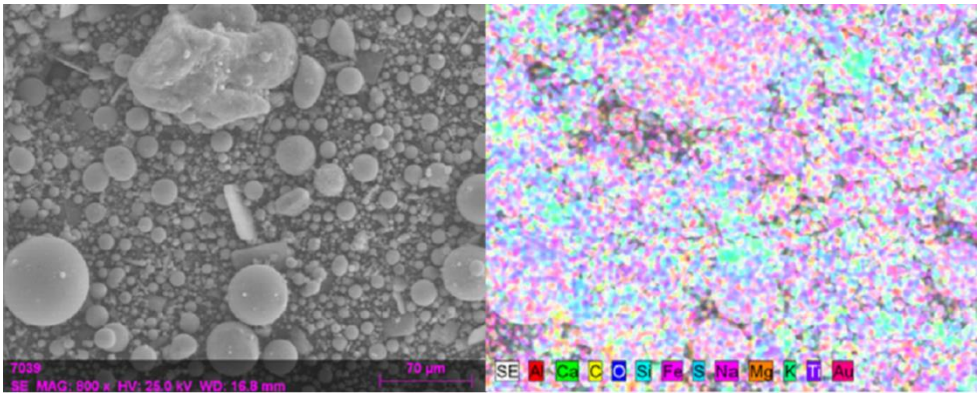


Fig. 10. SEM and SEM-EDX results for flotation column tailing

### Effect of mineralization method

In the bubble generator device shown in Fig. 11, a Venturi tube forms the bubbles in a cyclonic-static micro-bubble flotation column. For slurry at high pressure in the feed cell, it discharges through a nozzle at a high speed. Downstream of the nozzle, air was inhaled and crushed into micro-bubbles because of the negative pressure and high shear force. The results of the particle size analysis indicated that most of the unburned carbon was distributed in the fine particle fraction. Thus, the recovery of fine unburned carbon particles is important in removal of unburned carbon from coal fly ash. The micro-bubbles can increase the recovery of the fine particles by increasing the probability of collision and reducing the probability of detachment (Waters et al., 2008; Miettinen et al., 2010). Figure 12 shows the comparison of the bubbles from the froth zone formed in the FCSMC and the traditional flotation cell. It is obvious that the bubble size in FCSMC is much smaller than that in the traditional flotation cell and that the flotation foam is more stable in the FCSMC. Meanwhile, the high shear force in the bubble generator can strengthen the mineralization of the fine unburned carbon particles (Jameson, 2010). This conclusion indicates that pipe flow mineralization in FCSMC is superior for recovering fine unburned carbon from coal fly ash compared with the traditional flotation cell.

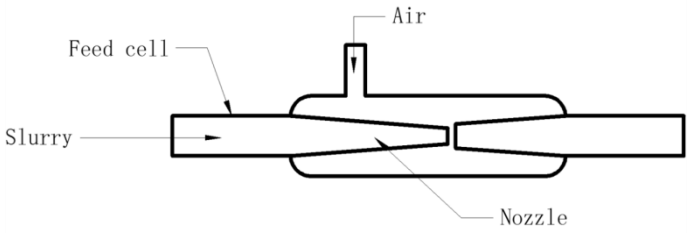


Fig. 11. Bubble generator of FCSMC

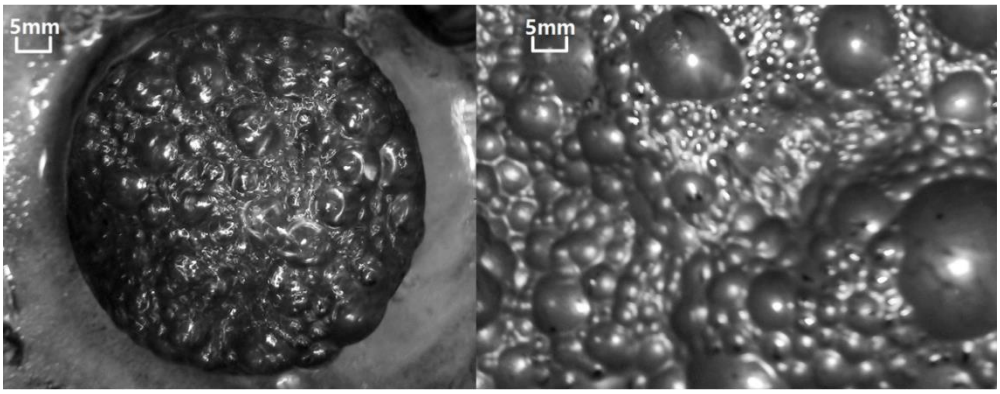


Fig. 12. Comparison of the bubbles from the froth zone formed in FCSMC and the traditional flotation cell

As shown in Fig. 13, a clear cyclone can be seen in the cyclonic separation section in the FCSMC under the condition of only tap water and no bubbles, indicating that the particle velocity can increase with the centrifugal acceleration. When the bubble generator inhales air, the relative velocity of the bubble-particle in FCSMC is higher than in the traditional flotation cell under a high intensity centrifugal force field. This increases the probability of collision between the particles and bubbles. Thus, the mineralization efficiency of flotation increases as the centrifugal force field accelerates. A high intensity centrifugal force field also can reduce the efficient flotation limit (Li et al., 2012), what means that the fine particles recovery increases with the centrifugal force field acceleration in FCSMC under a suitable centrifugal force range.

In the bubble generator, the high-pressure jet produce the micro-bubbles and strong turbulence pulp, which can strengthen the mineralization to increase the recovery of unburned carbon (Ucurum. 2009; Li et al., 2010). In cyclone flow, the strong turbulence, high relative velocity of the bubble-particle and localizes energy in the inner area of the cone where there are abundant bubbles, result that slowly floating minerals are forcibly recovered and tailings are effectively separated here (Yan et al., 2012; Deng et al., 2013). These advantages confirm that FCSCM is more suitable for removing unburned carbon from coal fly ash compared with the traditional flotation cell.

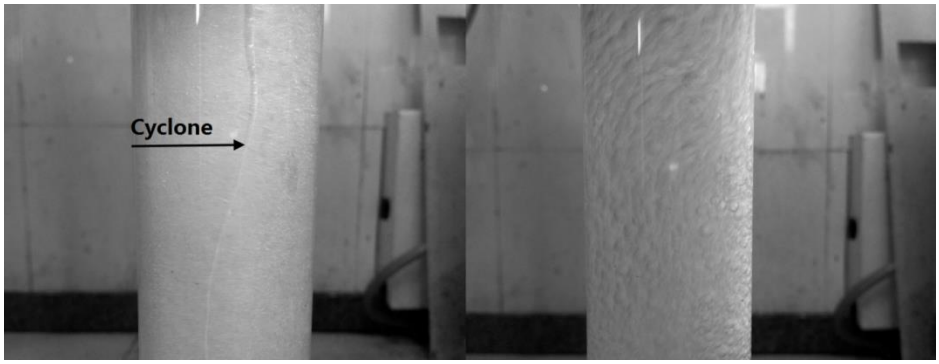


Fig. 13. Schematic illustration of cyclonic mineralization

## Conclusions

The performance of a cyclonic-static micro-bubble flotation column on the recovery of unburned carbon from the coal fly ash compared with a traditional flotation cell was investigated. Additionally, the effects of pipe-flow minimization and cyclonic minimization of FCSMC were analyzed. The conclusions drawn from this study are as follows.

1. Under optimum flotation conditions, the recovery of unburned carbon from the flotation column reached 89.69%, and was greater than 6.5% compared with the traditional flotation cell. $L_t$ for the flotation column decreased to 1.99%, and was lower than 1.1% compared with the traditional flotation cell.
2. The size and scanning electron microscope analyses demonstrated that the flotation column was beneficial for the recovery of fine particles. The yield of the −74 μm size fraction of the concentrates from the flotation column was higher than that of the traditional flotation cell by 6%.
3. FCSCM was more suitable for removing unburned carbon from coal fly ash compared with the traditional flotation cell, which was attributed to the pipe flow mineralization and cyclonic mineralization.

## Acknowledgements

The authors would like to thank the financial support from the Fundamental Research Funds for the Central Universities (China University of Mining and Technology), New Century Excellent Talents in University (Grant No. NCET-13-1020), the National Nature Science Foundation of China (Grant No. 51274198), and the Scientific Research Foundation for the Returned Overseas Chinese Scholars, State Education Ministry.

## References

ALTUN N.E., XIAO C.F., HWANG J.Y., 2009. *Separation of unburned carbon from fly ash using a concurrent flotation column.* Fuel Processing Technology, 90(12), 1464–1470.

ASOKAN P., SAXENA M., ASOLEKAR S.R., 2005. *Coal combustion residues environmental implications and recycling potentials*. Resources conservation and recycling, 43(3), 239–262.

CAO Y.J., GUI X.H., MA Z.L., YU X.X., CHEN X.D., ZHANG X.P., 2009. *Process mineralogy of copper-nickel sulphide flotation by a cyclonic-static micro-bubble flotation column*. Mining Science and Technology (China), 19(6), 784–787.

CHIPFUNHU D., ZANIN M., GRANO S., 2012. *Flotation behaviour of fine particles with respect to contact angle*. Chemical Engineering Research and Design, 90(1), 26–32.

DENG X.W., LIU J.T., WANG Y.T., CAO Y.J., 2013. *Velocity distribution of the flow field in the cyclonic zone of cyclone-static micro-bubble flotation column*. International Journal of Mining Science and Technology, 23(1), 89–94.

DEMIR U., YAMIK A., KELEBEK S., OTEYAKA B., UCAR A., SAHBAZ O., 2008. *Characterization and column flotation of bottom ashes from Tuncbilek power plant*. Fuel, 87(6), 666–672.

GURSOY Y. H., OTEYAKA B., 2015. *Effects of air-to-pulp ratio and bias factor on flotation of complex Cu-Zn sulphide ore in the Jameson cell*. Physicochemical problems of mineral processing, 51(2), 511-519.

HAN O.H., KIM B.G., KIM M.K., NIMAL S., PARK C.H., 2014. *Fine coal beneficiation by column flotation*. Fuel Processing Technology, 126, 49–59.

HUANG Y., TAKAOKA M., TAKEDA N., 2003. *Removal of unburned carbon from municipal solid waste fly ash by column flotation*, Waste Management, 23(4), 307-313.

JAMESON G.J., 2010. *New directions in flotation machine design*. Minerals Engineering, 23(11–13), 835–841.

KIANI A., ZHOU J., GALVIN K.P., 2015. *Enhanced recovery and concentration of positively buoyant cenospheres from negatively buoyant fly ash particles using the inverted reflux classifier*. Minerals Engineering, 79, 1–9.

KOWALCZUK P. B., MROCZKO D., DRZYMALA J., 2015. *Influence of frother type and dose on collectorless flotation of copper-bearing shale in a flotation column*. Physicochemical Problems of Mineral Processing, 51(2), 547-558.

LEE S., SEO M.D., KIM Y.J., PARK H.H., KIM T.N., HWANG Y., CHO S.B., 2010. *Unburned carbon removal effect on compressive strength development in a honeycomb briquette ash-based geopolymer*. International Journal of Mineral Processing, 97(1–4), 20-25.

LI G.S., CAO Y.J., LIU J.T., WANG D.P., 2012. *Cyclonic flotation column of siliceous phosphate ore*. International Journal of Mineral Processing, 110, 6–11.

LI L., LIU J.T., WANG W.Y., CAO Y.J., ZHANG H.J., YU H.S., 2009. *Experimental research on anionic reverse flotation of hematite with a flotation column*. Procedia Earth and Planetary Science, 1(1), 791–798.

LI L., LIU J.T., WANG L.J., YU H.H., 2010. *Numerical simulation of a self-absorbing microbubble generator for a cyclonic-static microbubble flotation column*. Mining Science and Technology (China), 20(1), 88-92.

MARTINEZ C.D., URIBE S.A., 2008. *An experimental study of the recovery of hydrophilic silica fines in column flotation*. Minerals Engineering, 21(15), 1102–1108.

MCCARTHY M.J., JONES M.R., ZHENG L., ROBL T.L., GROPPO J.G., 2013. *Characterising long-term wet-stored fly ash following carbon and particle size separation*. Fuel, 111, 430–441.

MIETTINEN T., RALSTON J., FORNASIERO D., 2010. *The limits of fine particle flotation*. Minerals Engineering, 23(5), 420–437.

NAKHAEI F., IRANNAJAD M., 2013. *Prediction of on-line froth depth measurement errors in industrial flotation columns: a promising tool for automatic control.* Physicochemical Problems of Mineral Processing, 49(2), 757-768.

OZDEMIR O., TARAN E., HAMPTON M.A., KARAKASHEV S.I., NGUYEN A.V., 2009. *Surface chemistry aspects of coal flotation in bore water*. International Journal of Mineral Processing, 92(3–4), 177–183.

PANG J.F., LI Q., WANG W., XU X.T., ZHAI J.P., 2011. *Preparation and characterization of electroless Ni–Co–P ternary alloy on fly ash cenospheres*. Surface and Coatings Technology, 205(17–18), 4237–4242.

SAHBAZ O., OTEYAKA B., KELEBEK S., UCAR A., DEMIR U., 2008. *Separation of unburned carbonaceous matter in bottom ash using Jameson cell.* Separation and Purification Technology, 62(1), 103-109.

SHAHBAZI B., REZAI B., JABAD KOLEINI S.M., 2010. *Bubble–particle collision and attachment probability on fine particles flotation*. Chemical Engineering and Processing: Process Intensification, 49(6), 622–627.

SPEARS D.A., 2000. *Role of clay minerals in UK coal combustion*. Applied Clay Science, 16(1–2), 87–95.

TAO D., LUTTRELL G.H., YOON R.H., 2000. *A parametric study of froth stability and its effect on column flotation of fine particles*. International Journal of Mineral Processing, 59(1), 25–43.

TASDEMIR T., TASDEMIR A., OTEYAKA B., 2011. *Gas entrainment rate and flow characterization in downcomer of a Jameson cell*. Physicochemical Problems of Mineral Processing, 47, 61-78.

UCAR A., SAHBAZ O., KERENCILER S., OTEYAKA, B., 2014. *Recycling of colemanite tailings using the Jameson flotation technology*. Physicochemical Problems of Mineral Processing, 50(2), 645-655.

UCURUM M., 2009. *Influences of Jameson flotation operation variables on the kinetics and recovery of unburned carbon.* Powder Technology, 191(3), 240–246.

WANG W., ZHAI J.P., LI Q., 2015. *Synthesis of buoyant metal-coated fly ash cenosphere and its excellent catalytic performance in dye degradation*. Journal of Colloid and Interface Science, 444, 10–16.

WATERS K.E., HADLER K., CILLIERS J.J., 2008. *The flotation of fine particles using charged microbubbles*. Minerals Engineering, 21(12–14), 918–923.

XIA W.C., YANG J.G., 2013. *Effect of pre-wetting time on oxidized coal flotation*. Powder Technology, 250, 63–66.

YAN X.K., LIU J.T., CAO Y.J., WANG L.J., 2012. *A single-phase turbulent flow numerical simulation of a cyclonic-static micro bubble flotation column*. International Journal of Mining Science and Technology, 22(1), 95-100.

ZHANG H.J., LIU J.T., WANG Y.T., CAO Y.J., MA Z.L., LI X.B., 2013. *Cyclonic-static micro-bubble flotation column*. Minerals Engineering, 45, 1–3.

ZOU W.J., CAO Y.J., LIU J.T., LI W.N., LIU C., 2013. *Wetting process and surface free energy components of two fine liberated middling bituminous coals and their flotation behaviors*, Powder Technology, 246, 669–676.